CURSHL: A HIGH-PRECISION FINITE ELEMENT FOR SHELLS OF ARBITRARY SHAPE

by

G.R. Cowper

A.H. Hall, Head,
Structures and Materials Section

F.R. Thurston
Director

SUMMARY

CURSHL is a high-precision finite element for the linear static stress analysis of thin elastic shells of quite general shape. The element is a fully-conforming displacement element of curvilinear triangular form. The theoretical basis of the element is presented in fairly complete detail, and some aspects of the organization of the computer program are discussed. The performance of CURSHL is examined with regard to accuracy of numerical integration, computation time, and representation of rigid-body modes.

TABLE OF CONTENTS

		Page
	SUMMARY	(iii)
	ILLUSTRATIONS	(v)
1.0	Introduction	1
2.0	Résumé of Formulas from Shell Theory	2
	2.1 Geometric Parameters	2
	2.2 Membrane and Bending Strains	5
	2.3 Stress-Strain Relations and Strain Energy	7
	2.4 Physical Components	9
3.0	Interpolation Functions for Displacements	11
	3.1 Local Coordinates	12
	3.2 Tangential Displacements	14
	3.3 Normal Displacement	16
4.0	Stiffness Matrix	22
	4.1 Outline of Calculation	22
	4.2 Evaluation of $\{e_i\}$	24
	4.3 Input Data for Matrices $[B]$ and $[E]$	25
	4.4 Efficient Calculation of Strain Energy Density	27
5.0	Load Vector	28
6.0	Performance of CURSHL	29
	6.1 Accuracy of Numerical Integration	29
	6.2 Computation Time	30
	6.3 Rigid Body Modes	30
7.0	References	32

TABLES

Table		Page
I	Strain-Displacement Matric $[B]$	34
II	Elasticity Matrix $[E]$	35
III	Transformation Matrices for Tangential Displacements	36
IV	Transformation Matrices for Normal Displacement	37
V	Numerical Integration Formula Used in CURSHL	38

TABLES (Cont'd)

Table		Page
VI	Transformation Matrix for Generalized Displacements	39
VII	Comparison of Solutions for Pressurized Spherical Cap	40
VIII	Computing Times for CURSHL	41
IX	Eigenvalues of KX = λMX, where K is the CURSHL Stiffness Matrix	42

ILLUSTRATIONS

Figure		Page
1	Local Coordinates	44
2	Positive Direction of Physical Components of Displacement and Rotation	45
3	Positive Directions of Physical Components of Stress Resultants and Bending Moments	46
4	Diagram of Spherical Cap. Uniform Applied Pressure	47

1.0 Introduction

CURSHL is the acronym both of a high-precision finite element for the static analysis of thin shells and of the associated computer program. The element is a fully conforming displacement element of curvilinear triangular shape which utilizes the same interpolation functions and generalized displacements as previous high-precision elements for plate bending, plane stress, shallow shells and cylindrical shells. Continuous Kirchoff constraints are used. The computer program generates the stiffness matrix and consistent load vector for a single element. Variable thickness and elastic modulus, as well as thermal loads, can be accommodated by the program but at present the program is limited to linear elastic isotropic material. The program provides the option of generating a stiffness matrix based on either Koiter-Sanders shell theory, Donnell-Vlasov shell theory, or shallow shell theory. Except for a requirement of smoothness the shape of the shell is virtually unrestricted.

A general description of CURSHL was first given at CANCAM '71 [10]*. An amplified description and an outline of the considerations which guided the development of CURSHL were given in Reference [1], which also included several examples of CURSHL's performance. Because the emphasis in these references was on the performance and accuracy of the element, many details of the theoretical and computational aspects were omitted. The purpose of the present report is to describe in fairly complete detail the underlying theory and to outline the organization of the computer program. In the pages which follow the relevant items from shell theory are presented, formulas for the interpolation of displacement within an element are derived, and the method of calculation of the stiffness matrix is described. In addition, certain computational details of the program are discussed. Finally, the element is tested in a small number of example problems

---

* Numbers in square brackets denote references at the end of the text.

in order to illustrate its accuracy.

2.0 Résumé of Formulas from Shell Theory

The required formulas from shell theory are assembled here for ease of reference. General tensor notation is used in order to avoid unnecessary restrictions on the shape of the shell or on coordinate systems. Of the multitude of existing first-order shell theories, the theory of Koiter-Sanders can claim, with reasonable justification, to be the best [4]. It is therefore used as the main theoretical basis of the element. It happens that the equations of the simplified theories of Donnell-Vlasov and of shallow shells are obtainable from the Koiter-Sanders equations by a few simple modifications. Since the latter theories are widely used, they are made optionally available in the computer program.

The treatise of Green and Zerna [2] is the source of the formulas for the geometric parameters, including the approximate formulas which may be used when the shell is shallow. The equations of Koiter-Sanders shell theory are taken from the papers of Koiter [3], and of Budiansky and Sanders[4]. Tensor notation following the conventions of Reference [2] is used throughout this section.

2.1 Geometric Parameters

(i) General Shell

Let θ_1, θ_2 be curvilinear coordinates on the shell's middle surface. Let the middle surface be defined by the position vector $\vec{r} = \vec{r}(\theta_1,\theta_2)$ whose Cartesian components are x, y, z. The covariant metric tensor is

$$a_{\lambda\mu} = \vec{r}_{,\lambda} \cdot \vec{r}_{,\mu} = x_{,\lambda}x_{,\mu} + y_{,\lambda}y_{,\mu} + z_{,\lambda}z_{,\mu} \qquad (2.1)$$

while the contravariant metric tensor is given by

$$a^{11} = a_{22}/a, \quad a^{12} = a^{21} = -a_{12}/a, \quad a^{22} = a_{11}/a \qquad (2.2)$$

where $$a = a_{11}a_{22} - a_{12}a_{21} \tag{2.3}$$

The unit normal vector is

$$\vec{n} = (\vec{r}_{,1} \times \vec{r}_{,2})/|\vec{r}_{,1} \times \vec{r}_{,2}| \tag{2.4}$$

and we note

$$|\vec{r}_{,1} \times \vec{r}_{,2}| = \sqrt{a} \tag{2.5}$$

The covariant and mixed curvature tensors are

$$b_{\lambda\mu} = \vec{n}\cdot\vec{r}_{,\lambda\mu} = n_x x_{,\lambda\mu} + n_y y_{,\lambda\mu} + n_z z_{,\lambda\mu} \tag{2.6}$$

$$b^{\lambda}_{\mu} = a^{\lambda\rho} b_{\mu\rho}$$

The contravariant base vectors are given by

$$\vec{a}^{\lambda} = a^{\lambda\rho}\vec{r}_{,\rho} \tag{2.7}$$

and the Christoffel symbols are

$$\Gamma^{\lambda}_{\mu\nu} = \vec{a}^{\lambda}\cdot\vec{r}_{,\mu\nu} = a^{\lambda\rho}\vec{r}_{,\rho}\cdot\vec{r}_{,\mu\nu} \tag{2.8}$$

$$= a^{\lambda\rho}(x_{,\rho}x_{,\mu\nu} + y_{,\rho}y_{,\mu\nu} + z_{,\rho}z_{,\mu\nu})$$

The formulas for covariant differentiation of first and second rank covariant tensors are

$$A_{\lambda|\mu} = A_{\lambda,\mu} - \Gamma^{\rho}_{\lambda\mu}A_{\rho} \tag{2.9}$$

$$A_{\lambda\mu|\nu} = A_{\lambda\mu,\nu} - \Gamma^{\rho}_{\lambda\nu}A_{\rho\mu} - \Gamma^{\rho}_{\mu\nu}A_{\rho\lambda} \tag{2.10}$$

In addition to the foregoing standard formulas, expressions for the covariant derivatives of the mixed curvature tensor are needed. To obtain these we first differentiate (2.6) to get

$$b_{\lambda\mu,\nu} = \vec{n}\cdot\vec{r}_{,\lambda\mu\nu} + \vec{n}_{,\nu}\cdot\vec{r}_{,\lambda\mu} \tag{2.11}$$

The derivatives of the normal vector are given by the Gauss-Weingarten formula

$$\vec{n}_{,\nu} = -b_{\nu}^{\tau}\vec{r}_{,\tau} = -a^{\tau\rho}b_{\nu\rho}\vec{r}_{,\tau} \tag{2.12}$$

so

$$\begin{aligned} b_{\lambda\mu,\nu} &= \vec{n}\cdot\vec{r}_{,\lambda\mu\nu} - a^{\tau\rho}\vec{r}_{,\tau}\cdot\vec{r}_{\lambda\mu}b_{\nu\rho} \\ &= \vec{n}\cdot\vec{r}_{,\lambda\mu\nu} - \Gamma^{\rho}_{\lambda\mu}b_{\nu\rho} \end{aligned} \tag{2.13}$$

Hence, from (2.10) and (2.13),

$$b_{\lambda\mu|\nu} = \vec{n}\cdot\vec{r}_{,\lambda\mu\nu} - \Gamma^{\rho}_{\lambda\mu}b_{\rho\nu} - \Gamma^{\rho}_{\lambda\nu}b_{\rho\mu} - \Gamma^{\rho}_{\mu\nu}b_{\rho\lambda} \tag{2.14}$$

It is interesting to note that $b_{\lambda\mu|\nu}$ is unaltered by any permutation of the indices. Since the covariant derivatives of the metric tensor vanish, the required formulas are

$$\begin{aligned} b^{\tau}_{\mu|\nu} &= a^{\lambda\tau}b_{\lambda\mu|\nu} \\ &= a^{\lambda\tau}(\vec{n}\cdot\vec{r}_{,\lambda\mu\nu} - \Gamma^{\rho}_{\lambda\mu}b_{\rho\nu} - \Gamma^{\rho}_{\lambda\nu}b_{\rho\mu} - \Gamma^{\rho}_{\mu\nu}b_{\rho\lambda}) \end{aligned} \tag{2.15}$$

(ii) Shallow Shell

When the shell is shallow certain approximations are permissible, as discussed in Section 11.3 of Reference [2]. The metric tensor of the shell can be approximated by the metric tensor of the base plane, and hence (2.1) is replaced by

$$a_{\lambda\mu} = x_{,\lambda}x_{,\mu} + y_{,\lambda}y_{,\mu} \tag{2.16}$$

The contravariant metric tensor is still given by (2.2) but now there is the alternative formula for a,

$$a = (x_{,1}y_{,2} - x_{,2}y_{,1})^2 \tag{2.17}$$

Hence, within the shallow shell approximation,

$$|\vec{r}_{,1} \times \vec{r}_{,2}| = \sqrt{a} = (x_{,1}y_{,2} - x_{,2}y_{,1}) \tag{2.18}$$

where the correct sign of the expression for $\sqrt{a}$ was determined from the particular case $\theta_1 = x, \theta_2 = y$.

The unit normal can still be calculated from (2.4), and in view of (2.18), the result agrees with the usual shallow shell approximation for the normal. That is, the z-component of $\vec{n}$ is 1 while the other two components are equal to the negative gradient of z. If, in turn, this result is used in (2.6) to calculate the curvature tensor the expressions obtained agree with the usual shallow shell approximation,

$$b_{\lambda\mu} = z||_{\lambda\mu} \tag{2.19}$$

where the double stroke denotes covariant differentiation in the base plane.

The Christoffel symbols for the base plane are obtained by replacing $\vec{r}$ in (2.8) by $\vec{R}$, where $\vec{R}$ is the component of $\vec{r}$ lying in the base plane, at the same time using (2.16) to calculate the metric tensor. Thus

$$\Gamma^{\lambda}_{\mu\nu} = a^{\lambda\rho}\vec{R}_{,\rho} \cdot \vec{R}_{,\mu\nu} = a^{\lambda\rho}(x_{,\rho}x_{,\mu\nu} + y_{,\rho}y_{,\mu\nu}) \tag{2.20}$$

In summary, for shallow shells formula (2.1) is replaced by (2.16) and formula (2.8) by (2.20), but the formulas for $a^{\lambda\mu}$, $\vec{n}$, and $b_{\lambda\mu}$ remain valid.

2.2 Membrane and Bending Strains

The membrane strain tensor is related to the displacements by

$$\begin{aligned} \varepsilon_{\lambda\mu} &= \tfrac{1}{2}(u_{\lambda|\mu} + u_{\mu|\lambda}) - b_{\lambda\mu}w \\ &= \tfrac{1}{2}(u_{\lambda,\mu} + u_{\mu,\lambda}) - \Gamma^{\rho}_{\lambda\mu}u_{\rho} - b_{\lambda\mu}w \end{aligned} \tag{2.21}$$

and this relation applies to all three of Koiter-Sanders, Donnell-Vlasov, and shallow shell theories.

In Koiter-Sanders theory the rotations of the normal ϕ_λ and the surface rotation $\omega_{\lambda\mu}$ are given by

$$\phi_\lambda = - w_{,\lambda} - b_\lambda^\rho u_\rho \tag{2.22}$$

$$\omega_{\lambda\mu} = \tfrac{1}{2}(u_{\lambda|\mu} - u_{\mu|\lambda}) = \tfrac{1}{2}(u_{\lambda,\mu} - u_{\mu,\lambda}) \tag{2.23}$$

and the bending strain tensor is

$$\begin{aligned}\kappa_{\lambda\mu} &= \tfrac{1}{2}(\phi_{\lambda|\mu} + \phi_{\mu|\lambda}) + \tfrac{1}{2}(b_\lambda^\rho \omega_{\mu\rho} + b_\mu^\rho \omega_{\lambda\rho}) \\ &= - w_{,\lambda\mu} + \Gamma_{\lambda\mu}^\rho w_{,\rho} \\ &\quad - \tfrac{3}{4}(b_\lambda^\rho u_{\rho,\mu} + b_\mu^\rho u_{\rho,\lambda}) + \tfrac{1}{4}(b_\lambda^\rho u_{\mu,\rho} + b_\mu^\rho u_{\lambda,\rho}) \\ &\quad + \tfrac{1}{2}(b_{\lambda|\mu}^\rho - b_{\mu|\lambda}^\rho + \Gamma_{\tau\mu}^\rho b_\lambda^\tau + \Gamma_{\tau\lambda}^\rho b_\mu^\tau) u_\rho\end{aligned} \tag{2.24}$$

In Donnell-Vlasov theory and in shallow shell theory the rotations of the normal are approximated by

$$\phi_\lambda = - w_{,\lambda} \tag{2.25}$$

and the bending strain tensor is given by the relatively simple formulas

$$\begin{aligned}\kappa_{\lambda\mu} &= \tfrac{1}{2}(\phi_{\lambda|\mu} + \phi_{\mu|\lambda}) = - w_{|\lambda\mu} \\ &= - w_{,\lambda\mu} + \Gamma_{\lambda\mu}^\rho w_{,\rho}\end{aligned} \tag{2.26}$$

These strain-displacement relations may be summarized by the matrix relation

$$\{e\} = [B]\{d\} \tag{2.27}$$

where {e} is a column vector of strains,

$$\{e\}^T = \{\varepsilon_{11}, \varepsilon_{12}, \varepsilon_{22}, \kappa_{11}, \kappa_{12}, \kappa_{22}\} \tag{2.28}$$

and {d} is a column vector of displacements and their derivatives,

$$\{d\}^T = \{u_1, u_{1,1}, u_{1,2}, u_2, u_{2,1}, u_{2,2}, w, w_{,1}, w_{,2}, w_{,11}, w_{,12}, w_{,22}\} \tag{2.29}$$

The matrix [B] is displayed in Table I.

2.3 Stress-Strain Relations and Strain Energy

The stress resultants and bending moments are related to the membrane and bending strains by

$$n^{\lambda\mu} = CH^{\lambda\mu\rho\tau}\varepsilon_{\rho\tau} \tag{2.30}$$

$$m^{\lambda\mu} = DH^{\lambda\mu\rho\tau}\kappa_{\rho\tau} \tag{2.31}$$

where C is the stretching rigidity, D the flexural rigidity, and

$$H^{\lambda\mu\rho\tau} = \tfrac{1}{2}\{(1-\nu)(a^{\lambda\tau}a^{\mu\rho} + a^{\lambda\rho}a^{\mu\tau}) + 2\nu a^{\lambda\mu}a^{\rho\tau}\} \tag{2.32}$$

For homogeneous shells of thickness t,

$$C = Et/(1-\nu^2), \qquad D = Et^3/12(1-\nu^2) \tag{2.33}$$

For laminated or sandwich shells other expressions for C and D may be appropriate and their use is not ruled out. However (2.30), (2.31), and (2.32) apply only to isotropic shells in which there is no coupling in the stress-strain relations between bending and stretching.

The strain energy density is

$$\begin{aligned} dU/dA &= \tfrac{1}{2}(n^{\lambda\mu}\varepsilon_{\lambda\mu} + m^{\lambda\mu}\kappa_{\lambda\mu}) \\ &= \tfrac{1}{2}(CH^{\lambda\mu\rho\tau}\varepsilon_{\lambda\mu}\varepsilon_{\rho\tau} + DH^{\lambda\mu\rho\tau}\kappa_{\lambda\mu}\kappa_{\rho\tau}) \end{aligned} \tag{2.34}$$

and this may be written in matrix shorthand as

$$dU/dA = \tfrac{1}{2}\{e\}^T[E]\{e\} \tag{2.35}$$

The matrix [E] is displayed in Table II.

When thermal expansion is considered the stress-strain relations are modified to

$$n^{\lambda\mu} = CH^{\lambda\mu\rho\tau}\varepsilon_{\rho\tau} - (E\tilde{\alpha}/(1-\nu))T_R a^{\lambda\mu} \tag{2.36}$$

$$m^{\lambda\mu} = DH^{\lambda\mu\rho\tau}\kappa_{\rho\tau} - (E\tilde{\alpha}/(1-\nu))T_M a^{\lambda\mu} \tag{2.37}$$

where $\tilde{\alpha}$ is the coefficient of thermal expansion and T_R and T_M are the resultant and the moment of the temperature T across the thickness. That is

$$T_R = \int_{-t/2}^{t/2} T(\zeta)d\zeta \tag{2.38}$$

$$T_M = \int_{-t/2}^{t/2} \zeta T(\zeta)d\zeta \tag{2.39}$$

where ζ is the coordinate in the thickness direction of the shell. Formulas (2.36) and (2.37) apply to homogeneous shells and would have to be modified for laminated and sandwich shells. The thermal strains do not affect the expression for strain energy, but instead influence the expression for the virtual work of the external loads.

We suppose that the shell is acted upon by a distributed load per unit area $\vec{p}$. The contravariant components of $\vec{p}$ are p^λ in the tangent plane and p^n normal to the shell. The virtual work per unit area of the applied loads, including the contribution of thermal effects, is

$$dV/dA = p^\lambda u_\lambda + p^n w + (E\tilde{\alpha}/(1-\nu))(T_R a^{\lambda\mu}\varepsilon_{\lambda\mu} + T_M a^{\lambda\mu}\varepsilon_{\lambda\mu}) \tag{2.40}$$

or, in matrix notation

$$dV/\alpha A = \{P\}^T\{d\} + \{Q\}^T\{e\} \tag{2.41}$$

where

$$\{P\}^T = \{p^1,0,0,p^2,0,0,p^n,0,0,0,0,0\} \tag{2.42}$$

$$\{Q\}^T = (E\tilde{\alpha}/(1-\nu))\{T_R a^{11},2T_R a^{12},T_R a^{22},T_M a^{11},2T_M a^{12},T_M a^{22}\} \tag{2.43}$$

2.4 Physical Components

The tensor components of stress or displacement are not the same as the physical components of these quantities. It is, of course, the physical components which are ultimately sought, although tensor components are used in setting up the stiffness matrix.

The physical components of displacement $\bar{u}$, $\bar{v}$, $\bar{w}$, resolved along the covariant base vectors, are related to the tensor components by

$$\begin{aligned} \bar{u} &= (a^{11}u_1 + a^{12}u_2)\sqrt{a_{11}} \\ \bar{v} &= (a^{12}u_1 + a^{22}u_2)\sqrt{a_{22}} \\ \bar{w} &= w \end{aligned} \tag{2.44}$$

The contravariant tensor components of load are related to the physical components $\bar{p}_1$, $\bar{p}_2$, $\bar{p}_n$, by

$$p^1 = \bar{p}_1/\sqrt{a_{11}}\ , \quad p^2 = \bar{p}_2/\sqrt{a_{22}}\ , \quad p^n = \bar{p}_n \tag{2.45}$$

The physical stress resultants $N_{\lambda\mu}$ and the physical bending moments $M_{\lambda\mu}$ are related to their tensor counterparts by

$$N_{11} = n^{11}\sqrt{(a_{11}/a^{11})}, \qquad N_{12} = n^{12}\sqrt{a}, \qquad N_{22} = n^{22}\sqrt{(a_{22}/a^{22})} \tag{2.46}$$

$$M_{11} = m^{11}\sqrt{(a_{11}/a^{11})}, \qquad M_{12} = m^{12}\sqrt{a}, \qquad M_{22} = m^{22}\sqrt{(a_{22}/a^{22})} \tag{2.47}$$

The physical components of the rotation of the normal $\bar{\phi}_1, \bar{\phi}_2$, are related to the tensor components by the formulas

$$\begin{aligned} \bar{\phi}_1 &= (a^{11}\phi_1 + a^{12}\phi_2)\sqrt{a_{11}} \\ \bar{\phi}_2 &= (a^{21}\phi_1 + a^{22}\phi_2)\sqrt{a_{22}} \end{aligned} \tag{2.48}$$

which are the same as the corresponding formulas for the displacements. According to Glockner [12] the physical component of the surface rotation Ω is given by

$$\begin{aligned} \Omega &= \epsilon^{\alpha\beta}\omega_{\beta\alpha}/2 \\ &= (u_{2,1} - u_{1,2})/2\sqrt{a} \end{aligned} \tag{2.49}$$

where $\epsilon^{\alpha\beta}$ is the alternating tensor.
We note in passing that the rotation vector $\vec{\Omega}$ is given by

$$\vec{\Omega} = \epsilon^{\alpha\beta}\phi_\alpha \vec{r}_{,\beta} + \Omega\vec{n} \tag{2.50}$$

The conventions for the positive directions of the physical components of displacement, rotation, stress resultants, and bending moments are illustrated in Figures 2 and 3. In the figures, the surface coordinates have been denoted as α, β, rather than θ_1, θ_2. The positive direction of the normal is such that the normal vector forms a right-handed triad with the tangent vectors along the α-curves and the β-curves. Figures 2 and 3 are intended to show non-orthogonal coordinates. The directions of the stress resultants are parallel to the coordinate curves. The vectors which represent the bending moments are orthogonal to the coordinate curves, and, consistent with this, the components of bending stress are parallel to the coordinate curves.

3.0 Interpolation Functions for Displacements

At this point we drop the tensor notation of the preceding section and introduce α,β to denote the general curvilinear coordinates on the shell surface, and u, v, w to denote the covariant tensor components of displacement. The coordinates α,β need not be principal nor orthogonal.

The curvilinear triangular element on the shell surface can be imagined mapped on to the α-β plane. The edges of the element are defined by specifying that they are straight lines in the α-β plane.

The displacements in CURSHL are interpolated by the same functions which have been used in previous high-precision elements [5,6,7,8]. The in-plane displacements u,v are taken as complete cubic polynomials in α,β, while w is taken as a restricted quintic polynomial in α,β. In keeping with this choice of displacement functions the generalized displacements are the values of u, $\partial u/\partial\alpha$, $\partial u/\partial\beta$, v, $\partial v/\partial\alpha$, $\partial v/\partial\beta$, w, $\partial w/\partial\alpha$, $\partial w/\partial\beta$, $\partial^2 w/\partial\alpha^2$, $\partial^2 w/\partial\alpha\partial\beta$, $\partial^2 w/\partial\beta^2$ at the three vertices of the element, for a total of 36 degrees of freedom. Centroidal displacements u_c, v_c, are used temporarily as degrees of freedom during the development of the stiffness matrix but are later eliminated by static condensation.

The choice of interpolation functions and generalized displacements assures that the element is fully conforming provided the shell surface satisfies certain smoothness conditions. For Koiter-Sanders theory these conditions are that the shell must be smooth and have continuous curvatures. For Donnell-Vlasov theory and for shallow shell theory it is sufficient that the shell is smooth. These conditions are discussed in more detail in References [1] and [7].

The order of the discretization error of a conforming finite element depends on the choice of interpolation functions, and can be predicted by the Taylor's series test introduced by

McLay [11]. The application of the test to the present element is essentially the same as in tests of previous high-precision elements for flat plates [5] and shallow shells [7]. The result is that the discretization error is of order h^5 where h is a typical linear dimension of an element. The Taylor's series test also shows that the interpolation functions for w on the one hand and for u,v on the other are matched, in the sense that they provide equal orders of accuracy in the strains.

Further discussion of the choice of interpolation functions is contained in Reference [1].

3.1 Local Coordinates

Let the vertices of the element be numbered 1,2,3 in counterclockwise order when viewed from the positive side of the element. Let the shell coordinates of the vertices be (α_1,β_1), (α_2,β_2), (α_3,β_3), respectively as shown in Figure 1.

In order to develop formulas relating the displacements within an element to the generalized displacements it is helpful to introduce a system of local oblique coordinates ξ,η. The ξ-axis is taken to coincide with the 1-2 edge of the element and the η-axis with the 1-3 edge, as shown in Figure 1. Further, the local coordinates are scaled so that ξ runs from 0 to 1 along edge 1-2 while η runs from 0 to 1 along edge 1-3. The relation between α,β and ξ,η is easily established as

$$\begin{aligned} \alpha &= \alpha_1 + (\alpha_2-\alpha_1)\xi + (\alpha_3-\alpha_1)\eta \\ \beta &= \beta_1 + (\beta_2-\beta_1)\xi + (\beta_3-\beta_1)\eta \end{aligned} \tag{3.1}$$

Derivatives with respect to local and global coordinates are related by

$$
\begin{aligned}
\partial/\partial\xi &= f_{11}\partial/\partial\alpha + f_{21}\partial/\partial\beta \\
\partial/\partial\eta &= f_{12}\partial/\partial\alpha + f_{22}\partial/\partial\beta \\
\partial^2/\partial\xi^2 &= f_{11}^2\partial^2/\partial\alpha^2 + 2f_{11}f_{21}\partial^2/\partial\alpha\partial\beta + f_{21}^2\partial^2/\partial\beta^2 \\
\partial^2/\partial\xi\partial\eta &= f_{11}f_{12}\partial^2/\partial\alpha^2 + (f_{11}f_{22} + f_{21}f_{12})\partial^2/\partial\alpha\partial\beta + f_{21}f_{22}\partial^2/\partial\beta^2 \\
\partial^2/\partial\eta^2 &= f_{12}^2\partial^2/\partial\alpha^2 + 2f_{12}f_{22}\partial^2/\partial\alpha\partial\beta + f_{22}^2\partial^2/\partial\beta^2
\end{aligned}
\tag{3.2}
$$

$$
\begin{aligned}
\partial/\partial\alpha &= d_{11}\partial/\partial\xi + d_{21}\partial/\partial\eta \\
\partial/\partial\beta &= d_{12}\partial/\partial\xi + d_{22}\partial/\partial\eta \\
\partial^2/\partial\alpha^2 &= d_{11}^2\partial^2/\partial\xi^2 + 2d_{11}d_{21}\partial^2/\partial\xi\partial\eta + d_{21}^2\partial^2/\partial\eta^2 \\
\partial^2/\partial\alpha\partial\beta &= d_{11}d_{12}\partial^2/\partial\xi^2 + (d_{11}d_{22} + d_{21}d_{12})\partial^2/\partial\xi\partial\eta + d_{21}d_{22}\partial^2/\partial\eta^2 \\
\partial^2/\partial\beta^2 &= d_{12}^2\partial^2/\partial\xi^2 + 2d_{12}d_{22}\partial^2/\partial\xi\partial\eta + d_{22}^2\partial^2/\partial\eta^2
\end{aligned}
\tag{3.3}
$$

where

$$
\begin{aligned}
f_{11} &= \alpha_2 - \alpha_1 & f_{12} &= \alpha_3 - \alpha_1 \\
f_{21} &= \beta_2 - \beta_1 & f_{22} &= \beta_3 - \beta_1
\end{aligned}
$$

$$
\begin{aligned}
d_{11} &= (\beta_3 - \beta_1)/f & d_{12} &= -(\alpha_3 - \alpha_1)/f \\
d_{21} &= -(\beta_2 - \beta_1)/f & d_{22} &= (\alpha_2 - \alpha_1)/f
\end{aligned}
\tag{3.4}
$$

$$
f = (\alpha_2 - \alpha_1)(\beta_3 - \beta_1) - (\alpha_3 - \alpha_1)(\beta_2 - \beta_1)
$$

The Jacobian of the transformation is equal to f,

$$
\frac{\partial(\alpha,\beta)}{\partial(\xi,\eta)} = f \tag{3.5}
$$

3.2 Tangential Displacements

The tangential displacement u is taken as a complete cubic polynomial in the shell coordinates α,β, or equivalently as a complete cubic polynomial in the local coordinates, thus

$$u = a_1 + a_2\xi + a_3\eta + a_4\xi^2 + a_5\xi\eta + a_6\eta^2 + a_7\xi^3 + a_8\xi^2\eta + a_9\xi\eta^2 + a_{10}\eta^3 \tag{3.6}$$

The corresponding generalized displacements are the values of u and its first derivatives with respect to α,β at the three vertices of the element. In order to match the number of generalized displacements with the number of coefficients in (3.6) the displacement u_c at the centroid is introduced as an additional generalized displacement. Later u_c will be eliminated by static condensation.

Denote the values of u, $\partial u/\partial\xi$, etc. at vertex number 1 by u_1, $u_{\xi 1}$, etc. Since the local coordinates of vertices 1,2,3, and of the centroid are (0,0), (1,0), (0,1), (1/3,1/3), respectively, the following relations are obtained from (3.6)

$$\begin{aligned}
u_1 &= a_1 \\
u_{\xi 1} &= a_2 \\
u_{\eta 1} &= a_3 \\
u_2 &= a_1 + a_2 + a_4 + a_7 \\
u_{\xi 2} &= a_2 + 2a_4 + 3a_7 \\
u_{\eta 2} &= a_3 + a_5 + a_8 \\
u_3 &= a_1 + a_3 + a_6 + a_{10} \\
u_{\xi 3} &= a_2 + a_5 + a_9 \\
u_{\eta 3} &= a_3 + 2a_6 + 3a_{10} \\
u_c &= a_1 + (a_2+a_3)/3 + (a_4+a_5+a_6)/9 + (a_7+a_8+a_9+a_{10})/27
\end{aligned} \tag{3.7}$$

These relations may be explicitly inverted to give

$$\{A_u\} = [T_u]\{W_u'\} \tag{3.8}$$

where $\{A_u\}$, $\{W_u'\}$ are the column vectors

$$\{A_u\}^T = \{a_1, a_2, a_3, \ldots a_{10}\} \tag{3.9}$$

$$\{W_u'\}^T = \{u_1, u_{\xi 1}, u_{\eta 1}, u_2, u_{\xi 2}, u_{\eta 2}, u_3, u_{\xi 3}, u_{\eta 3}, u_c\} \tag{3.10}$$

and the matrix $[T_u]$ is displayed in Table III.

Let $\{W_u\}$ be the column vector of generalized displacements

$$\{W_u\}^T = \{u_1, u_{1\alpha}, u_{1\beta}, u_2, u_{2\alpha}, u_{2\beta}, u_3, u_{3\alpha}, u_{3\beta}, u_c\} \tag{3.10a}$$

where $u_{1\alpha}$, etc. denotes the value of $\partial u/\partial\alpha$ at vertex number 1, etc. The relation between $\{W_u\}$ and $\{W_u'\}$ is evident from equations (3.2) and may be written in matrix form as

$$\{W_u'\} = [R_u]\{W_u\} \tag{3.11}$$

where $[R_u]$ is given in Table III. Hence the polynomial coefficients of (3.6) are related to the generalized displacements by

$$\{A_u\} = [T_u][R_u]\{W_u\} \tag{3.12}$$

Given the generalized displacements, the polynomial coefficients can be calculated from (3.12) and, in turn, the values of u and its derivatives can be found from (3.6). A similar relation applies to the displacement v.

An advantage of using local coordinates is that $[T_u]$ can be found explicitly and is simple in form.

3.3 Normal Displacement

The normal displacement w is taken as a quintic polynomial,

$$w = b_1 + b_2\xi + b_3\eta + b_4\xi^2 + \ldots + b_{20}\xi\eta^4 + b_{21}\eta^5 \qquad (3.13)$$

As in previous high-precision elements, constraints are imposed on (3.13) to restrict the derivative of w in the direction perpendicular to any edge to a cubic variation along the edge.

The notation $w_1, w_{\xi 1}$, etc. is used to denote the values of w, $\partial w/\partial \xi$, etc. at vertex 1, and so on. The following relations involving twelve of the polynomial coefficients are obtained directly from (3.13)

$$\begin{aligned}
w_1 &= b_1 \\
w_{\xi 1} &= b_2 \\
w_{\eta 1} &= b_3 \\
w_{\xi\xi 1} &= 2b_4 \\
w_{\xi\eta 1} &= b_5 \\
w_{\eta\eta 1} &= 2b_6 \qquad (3.14) \\
w_2 &= b_1 + b_2 + b_4 + b_7 + b_{11} + b_{16} \\
w_{\xi 2} &= b_2 + 2b_4 + 3b_7 + 4b_{11} + 5b_{16} \\
w_{\xi\xi 2} &= 2b_4 + 6b_7 + 12b_{11} + 20b_{16} \\
w_3 &= b_1 + b_3 + b_6 + b_{10} + b_{15} + b_{21} \\
w_{\eta 3} &= b_3 + 2b_6 + 3b_{10} + 4b_{15} + 5b_{21} \\
w_{\eta\eta 3} &= 2b_6 + 6b_{10} + 12b_{15} + 20b_{21}
\end{aligned}$$

These relations can be explicitly inverted to give

$$
\begin{aligned}
b_1 &= w_1 \\
b_2 &= w_{\xi 1} \\
b_3 &= w_{\eta 1} \\
b_4 &= w_{\xi\xi 1}/2 \\
b_5 &= w_{\xi\eta 1} \\
b_6 &= w_{\eta\eta 1}/2 \\
b_7 &= -10w_1 - 6w_{\xi 1} - (3/2)w_{\xi\xi 1} + 10w_2 - 4w_{\xi 2} + w_{\xi\xi 2}/2 \\
b_{10} &= -10w_1 - 6w_{\eta 1} - (3/2)w_{\eta\eta 1} + 10w_3 - 4w_{\eta 3} + w_{\eta\eta 3}/2 \\
b_{11} &= 15w_1 + 8w_{\xi 1} + (3/2)w_{\xi\xi 1} - 15w_2 + 7w_{\xi 2} - w_{\xi\xi 2} \\
b_{15} &= 15w_1 + 8w_{\eta 1} + (3/2)w_{\eta\eta 1} - 15w_3 + 7w_{\eta 3} - w_{\eta\eta 3} \\
b_{16} &= -6w_1 - 3w_{\xi 1} - w_{\xi\xi 1}/2 + 6w_2 - 3w_{\xi 2} + w_{\xi\xi 2}/2 \\
b_{21} &= -6w_1 - 3w_{\eta 1} - w_{\eta\eta 1}/2 + 6w_3 - 3w_{\eta 3} + w_{\eta\eta 3}/2
\end{aligned}
\tag{3.15}
$$

To obtain formulas for the other coefficients, the constraints on the derivatives of w must be considered. Since terms of quartic and lower degree give first derivatives which vary at most cubically, the constraints affect only the six quintic terms in (3.13).

With reference to Figure 1, the derivative in the direction perpendicular to the edge 1-2 in the α-β plane is given by

$$\partial w/\partial n = \sin\theta\ \partial w/\partial\alpha - \cos\theta\ \partial w/\partial\beta \tag{3.16}$$

where

$$\sin\theta = (\beta_2-\beta_1)/\sqrt{s_{33}}, \quad \cos\theta = (\alpha_2-\alpha_1)/\sqrt{s_{33}}$$
$$s_{33} = (\alpha_2-\alpha_1)^2 + (\beta_2-\beta_1)^2 \tag{3.17}$$

Transforming (3.16) to derivatives with respect to ξ,η gives, after some manipulation

$$\partial w/\partial n = \{s_{32}\partial w/\partial\xi - s_{33}\partial w/\partial\eta\}/(f\sqrt{s_{33}}) \tag{3.18}$$

where

$$s_{32} = (\alpha_2-\alpha_1)(\alpha_3-\alpha_1) + (\beta_2-\beta_1)(\beta_3-\beta_1) \tag{3.19}$$

On edge 1-2, on which $\eta=0$, the contribution to the term in parentheses in (3.18) from the quintic terms in (3.13) is simply

$$(5s_{32}b_{16}-s_{33}b_{17})\xi^4 \tag{3.20}$$

and hence the condition for cubic variation of the derivative perpendicular to the edge 1-2 is

$$b_{17} = (5s_{32}/s_{33})b_{16} \tag{3.21}$$

The above equation determines b_{17} since b_{16} is already known from (3.15).

Similarly, the constraint along the edge 1-3 leads to the result

$$b_{20} = (5s_{32}/s_{22})b_{21} \tag{3.22}$$

where

$$s_{22} = (\alpha_3-\alpha_1)^2 + (\beta_3-\beta_1)^2 \tag{3.23}$$

The constraint along the edge 2-3 leads to the equation

$$s_{21}(5b_{16}-4b_{17}+3b_{18}-2b_{19}+b_{20}) = s_{31}(b_{17}-2b_{18}+3b_{19}-4b_{20}+5b_{21}) \tag{3.24}$$

where

$$s_{21} = (\alpha_3-\alpha_1)(\alpha_3-\alpha_2) + (\beta_3-\beta_1)(\beta_3-\beta_2)$$
$$s_{31} = (\alpha_2-\alpha_1)(\alpha_3-\alpha_2) + (\beta_2-\beta_1)(\beta_3-\beta_2) \qquad (3.25)$$

The following four relations are obtained directly from (3.13)

$$w_{\eta 2} = b_3 + b_5 + b_8 + b_{12} + b_{17}$$
$$w_{\xi\eta 2} = b_5 + 2b_8 + 3b_{12} + 4b_{17}$$
$$w_{\xi 3} = b_2 + b_5 + b_9 + b_{14} + b_{20} \qquad (3.26)$$
$$w_{\xi\eta 3} = b_5 + 2b_9 + 3b_{14} + 4b_{20}$$

and these can be solved to give b_8, b_{12}, b_9, b_{14} in terms of quantities already known,

$$b_8 = -3w_{\eta 1} - 2w_{\xi\eta 1} + 3w_{\eta 2} - w_{\xi\eta 2} + b_{17}$$
$$b_{12} = 2w_{\eta 1} + w_{\xi\eta 1} - 2w_{\eta 2} + w_{\xi\eta 2} - 2b_{17} \qquad (3.27)$$
$$b_9 = -3w_{\xi 1} - 2w_{\xi\eta 1} + 3w_{\xi 3} - w_{\xi\eta 3} + b_{20}$$
$$b_{14} = 2w_{\xi 1} + w_{\xi\eta 1} - 2w_{\xi 3} + w_{\xi\eta 3} - 2b_{20}$$

To determine the remaining coefficients b_{13}, b_{18}, b_{19}, there are the relations obtained from (3.13)

$$w_{\xi\xi 3} = 2(b_4+b_8+b_{13}+b_{19})$$
$$w_{\eta\eta 2} = 2(b_6+b_9+b_{13}+b_{18}) \qquad (3.28)$$

and the constraint equation (3.24). Solution of these equations, making use of (3.21) and (3.22) gives the results

$$b_{13} = -(2s_{21}+3s_{31})w_{\xi\xi 3}/2s_{11} + (3s_{21}+2s_{31})w_{\eta\eta 2}/2s_{11}$$
$$+ (2s_{21}+3s_{31})(b_4+b_8)/s_{11} + (3s_{21}+2s_{31})(b_6+b_9)/s_{11}$$
$$- (A_1/s_{11})b_{16} - (A_2/s_{11})b_{17} \qquad (3.29)$$

$$b_{18} = w_{\eta\eta 2}/2 - b_6 - b_9 - b_{13}$$

$$b_{19} = w_{\xi\xi 3}/2 - b_4 - b_8 - b_{13}$$

where

$$s_{11} = (\alpha_3-\alpha_2)^2 + (\beta_3-\beta_2)^2$$
$$s_{21} = (\alpha_3-\alpha_1)(\alpha_3-\alpha_2) + (\beta_3-\beta_1)(\beta_3-\beta_2)$$
$$s_{31} = (\alpha_2-\alpha_1)(\alpha_3-\alpha_2) + (\beta_2-\beta_1)(\beta_3-\beta_2) \qquad (3.30)$$
$$A_1 = -5s_{21} + 5(4s_{21}+s_{31})s_{32}/s_{33}$$
$$A_2 = -5(s_{21}+4s_{31})s_{32}/s_{22} + 5s_{31}$$

In obtaining the above results, the fact $s_{11} = s_{21}-s_{31}$ was used.

The connection between the polynomial coefficients b_i and the nodal values of w and its derivatives can be expressed in matrix form

$$\{A_w\} = [T_w]\{W'_w\} \qquad (3.31)$$

where

$$\{A_w\}^T = \{b_1, b_2, b_3, \ldots, b_{21}\} \qquad (3.32)$$

$$\{W'_w\}^T = \{w_1, w_{\xi 1}, w_{\eta 1}, w_{\xi\xi 1}, w_{\xi\eta 1}, w_{\eta\eta 1}, w_2, \ldots, w_3, \ldots\} \qquad (3.33)$$

In the computer program the matrix $[T_w]$ is set up in the following way. First, the terms in twelve of the rows of $[T_w]$ are implied by the relations (3.15) and these terms are inserted into the matrix. In view of the relations $b_{17} = (5s_{32}/s_{33})b_{16}$ and $b_{20} = (5s_{32}/s_{22})b_{21}$ the rows 17 and 21 of $[T_w]$ are respectively equal to row 16 multiplied by $(5s_{32}/s_{33})$ and to row 21

multiplied by $(5s_{32}/s_{22})$. The coefficient b_8 is given by the first of formulas (3.27), that is by

$$b_8 = - 3w_{\eta 1} - 2w_{\xi\eta 1} + 3w_{\eta 2} - w_{\xi\eta 2} + b_{17}$$

Hence to set up row 8 of $[T_w]$, numbers are first inserted into this row corresponding to the relation

$$b_8 = - 3w_{\eta 1} - 2w_{\xi\eta 1} + 3w_{\eta 2} - w_{\xi\eta 2}$$

and then row 17 is added to row 8. The remaining rows 9,12,13, 14,18,19, are set up in a similar way using relations (3.27) and (3.29).

Let $\{W_w\}$ be the column vector of generalized displacements

$$\{W_w\}^T = \{w_1, w_{1\alpha}, w_{1\beta}, w_{1\alpha\alpha}, w_{1\alpha\beta}, w_{1\beta\beta}, w_2, \ldots, w_3, \ldots\} \qquad (3.34)$$

where w_{1_α} etc. denotes the value of $\partial w/\partial\alpha$ at vertex number 1. The relation between $\{W_w\}$ and $\{W_w'\}$ is evident from equations (3.2) and may be written in matrix form as

$$\{W_w'\} = [R_w]\{W_w\} \qquad (3.35)$$

where $[R_w]$ is displayed in Table IV. Hence the polynomial coefficients of (3.13) are related to the generalized displacements by

$$\{A_w\} = [T_w][R_w]\{W_w\} \qquad (3.36)$$

Although $[T_w]$ has not been written down explicitly, its calculation is simple and requires no matrix inversion.

4.0 Stiffness Matrix

4.1 Outline of Calculation

The expression for strain energy density in a shell was presented in section 2.3. The strain energy of the finite element therefore is

$$U_e = \tfrac{1}{2}\int\int\{e\}^T[E]\{e\}\sqrt{a}\,d\alpha d\beta \tag{4.1}$$

where $\sqrt{a}\,d\alpha d\beta$ is the differential of area on the shell surface. The terms of the stiffness matrix [K] can be obtained from (4.1) by noting that the i-jth term of [K] is given by

$$k_{ij} = \partial^2 U_e/\partial X_i \partial X_j \tag{4.2}$$

where X_i denotes the i-th generalized displacement. With the notation

$$\{e_i\} = \partial\{e\}/\partial X_i \tag{4.3}$$

differentiation of (4.1) gives, in view of the symmetry of [E],

$$k_{ij} = \int\int\{e_i\}^T[E]\{e_j\}\sqrt{a}\,d\alpha d\beta \tag{4.4}$$

Since the strains depend linearly on the displacements u,v,w, which in turn are linearly proportional to the generalized displacements X_i, the quantity $\{e_i\}$ may be interpreted as the strains which occur when the i-th generalized displacement has unit value and all other generalized displacements are zero. The evaluation of $\{e_i\}$ will be discussed later.

When the integration is transformed to local coordinates formula (4.4) becomes

$$k_{ij} = \int\int\{e_i\}^T[E]\{e_j\}f\sqrt{a}\,d\alpha d\beta \tag{4.5}$$

where f is the Jacobian of the transformation. The strains which appear in the integrand of (4.5) depend in a complex way on the shell's curvature, its metric tensor, and the Christoffel symbols. The latter quantities can be complicated functions of the shell coordinates. Rather than attempt to approximate them by polynomials, thus making closed-form evaluation of (4.5) possible, it seems more convenient to evaluate (4.5) by numerical integration.

The use of numerical integration introduces a certain error. In order not to degrade the accuracy of the high-precision element, the error in the numerical integration formula should not be worse than h^6, which is the order of the discretization error. In fact, a formula with an error of order h^8 is used, in an attempt to make the error of numerical integration negligible. Details of the formula, which is a 13-point quadrature formula of Gaussian type, are given in Table V and Reference [9]. The formula is fully symmetric with respect to the three vertices. Application of the formula is facilitated by the fact that the local coordinates ξ,η are two of the three area coordinates of points within the triangle while the third area coordinate is $1-\xi-\eta$.

When numerical integration is applied to (4.5) the formula becomes

$$k_{ij} = \tfrac{1}{2} \sum_{n} c_n \left(\{e_i\}^T[E]\{e_j\}f\sqrt{a}\right)_n \qquad (4.6)$$

where the subscript n on the bracketted quantity indicates that the quantity is to be evaluated at the n-th pivotal point of the numerical integration. It is this formula which is the basis of the calculation of the stiffness matrix. The sequence of calculation is as follows. At the first pivotal point of the numerical integration the geometric parameters of the shell are computed and the column vector $\{e_i\}$ is evaluated for each i and stored. Then the expression $\frac{1}{2}\{e_i\}^T[E]\{e_j\}f\sqrt{a}$ is computed for all i and j, is multiplied by the weighting factor c_n of the numerical

integration, and the results are stored in the array which the completed stiffness matrix will eventually occupy. The procedure is then repeated at the second pivotal point of the numerical integration and the results are added term-by-term to the quantities which already occupy the stiffness matrix array. The procedure is then repeated at the third pivotal point and continues until all pivotal points have been covered. In this way the uncondensed stiffness matrix is built up. The final step is to statically condense the stiffness matrix so as to eliminate the centroidal displacements.

The foregoing sequence of calculations seems to be as economical as any, both in regard to storage space and number of operations.

4.2 Evaluation of $\{e_i\}$

It was shown in section 2.2 that $\{e\}$ is related to the vector of displacements and their derivatives $\{d\}$ by

$$\{e\} = [B]\{d\} \tag{4.7}$$

where, in the notation of the present section

$$\{d\}^T = \{u, u_\alpha, u_\beta, v, v_\alpha, v_\beta, w, w_\alpha, w_\beta, w_{\alpha\alpha}, w_{\alpha\beta}, w_{\beta\beta}\} \tag{4.8}$$

the subscripts denoting derivatives with respect to α and β. We define the corresponding vector $\{d'\}$ involving derivatives with respect to ξ and η,

$$\{d'\}^T = \{u, u_\xi, u_\eta, v, v_\xi, v_\eta, w, w_\xi, w_\eta, w_{\xi\xi}, w_{\xi\eta}, w_{\eta\eta}\} \tag{4.9}$$

From equations (3.3) the relation between $\{d\}$ and $\{d'\}$ is

$$\{d\} = [R_d]\{d'\} \tag{4.10}$$

where $[R_d]$ is given in Table VI. Hence

$$\{e\} = [B][R_d]\{d'\} \tag{4.11}$$

and therefore

$$\{e_i\} = [B][R_d]\{d_i'\} \tag{4.12}$$

where $\{d_i'\}$ is defined as

$$\{d_i'\} = \partial\{d\}/\partial X_i \tag{4.13}$$

Since the displacements are linearly proportional to the generalized displacements, $\{d_i'\}$ can be interpreted as the value of $\{d'\}$ when the i-th generalized displacement has unit value and the other generalized displacements are zero.

The procedure for finding $\{e_i\}$ then is the following. The i-th generalized displacement is given unit value and all other generalized displacements are set equal to zero. The corresponding polynomial coefficients are calculated, from (3.12) and (3.36). The values of displacement and their derivatives, in other words the value of $\{d_i\}$, are then calculated from the polynomial interpolation functions. Finally $\{e_i\}$ is obtained from (4.12).

4.3 Input Data for Matrices [B] and [E]

The matrices [B] and [E] depend in a very complex way on the geometric parameters of the shell. In general these parameters vary over the shell surface, and hence [B] and [E] must be evaluated at each pivotal point of the numerical integration.

As assumed in section 2.1, the shape of the shell is specified by giving the position vector $\vec{r}$ as a function of the shell coordinates

$$\vec{r} = \vec{r}\,(\alpha,\beta)$$

or, in component form, by specifying

$$x = x(\alpha,\beta), \qquad y = y(\alpha,\beta), \qquad z = z(\alpha,\beta)$$

where x,y,z, are the Cartesian components of $\vec{r}$. By using the formulas of section 2.1 all terms of [B] can be computed if the values of x,y,z and their derivatives are known. Derivatives up to third order are required in Koiter-Sanders theory while second order derivatives suffice for Donnell-Vlasov and shallow shell theory. This data is fed into the computer program from a user-supplied subroutine which must return the values of x,y,z, and their derivatives at an arbitrarily given point α,β. If, as is generally the case, the shell surface is of simple form then the exact equations of the surface can be used in setting up the subroutine. On the other hand the representation of the shell by a fitted polynomial surface is not precluded.

The computer program incorporates switches to evaluate [B] according to either of the three shell theories.

The matrix [E] depends not only on the geometric parameters but also on the elastic parameters C,D, and ν. Since numerical integration is used, variable thickness and elastic moduli can be handled easily. It is only necessary to use the appropriate values of C,D, and ν at each pivotal point of the numerical integration. This data is fed into the computer program from a second user-supplied subroutine which must return the values of C,D, and ν at any arbitrarily given point α,β. This method of handling the input data accommodates variable elastic properties but still is fairly simple in the case of constant properties.

4.4 Efficient Calculation of Strain Energy Density

In the computer program the calculation of the expression $\frac{1}{2}c_n(\{e_i\}^T[E]\{e_j\}f\sqrt{a})_n$ in (4.6) occurs within a triple do-loop, the loops spanning the rows of the stiffness matrix, the columns of the stiffness matrix, and the pivotal points of the numerical integration. Consequently each operation performed in evaluating the expression is repeated some 9600 times. It is therefore good to reduce the number of operations to a minimum.

If the expression is multiplied out it is found that it can be reduced to

$$\begin{aligned}\tfrac{1}{2}c_n\{e_i\}^T[E]\{e_j\}f\sqrt{a} &= \tfrac{1}{2}fc_nC(\varepsilon^i\varepsilon^j\sqrt{a} + ((1-\nu)/\sqrt{a})(2\varepsilon^i_{12}\varepsilon^j_{12} - \varepsilon^i_{11}\varepsilon^j_{22} - \varepsilon^i_{22}\varepsilon^j_{11})) \\ &+ \tfrac{1}{2}fc_nD(\kappa^i\kappa^j\sqrt{a} + ((1-\nu)/\sqrt{a})(2\kappa^i_{12}\kappa^j_{12} - \kappa^i_{11}\kappa^j_{22} - \kappa^i_{22}\kappa^j_{11}))\end{aligned} \tag{4.14}$$

where

$$\begin{aligned}\varepsilon^i &= a^{11}\varepsilon^i_{11} + 2a^{12}\varepsilon^i_{12} + a^{22}\varepsilon^i_{22} \\ \kappa^i &= a^{11}\kappa^i_{11} + 2a^{12}\kappa^i_{12} + a^{22}\kappa^i_{22}\end{aligned} \tag{4.15}$$

and where the superscript i denotes the components of $\{e_i\}$. That is

$$\{e_i\}^T = \{e^i_{11}, \varepsilon^i_{12}, \varepsilon^i_{22}, \kappa^i_{11}, \kappa^i_{12}, \kappa^i_{22}\} \tag{4.16}$$

If we define

$$\begin{aligned}\bar{\varepsilon}^i_{11} &= \sqrt{((1-\nu)c_nCf/2\sqrt{a})}\varepsilon^i_{11} \\ \bar{\varepsilon}^i_{22} &= \sqrt{((1-\nu)c_nCf/2\sqrt{a})}\varepsilon^i_{22} \\ \bar{\varepsilon}^i_{12} &= \sqrt{((1-\nu)c_nCf/\sqrt{a})}\varepsilon^i_{12} \\ \bar{\varepsilon}^i &= \sqrt{(c_nCf\sqrt{a}/2)}\varepsilon^i\end{aligned} \tag{4.17}$$

$$\begin{aligned}
\bar{\kappa}^i_{11} &= \sqrt{((1-\nu)c_n Df/2\sqrt{a})}\kappa^i_{11} \\
\bar{\kappa}^i_{22} &= \sqrt{((1-\nu)c_n Df/2\sqrt{a})}\kappa^i_{22} \\
\bar{\kappa}^i_{12} &= \sqrt{((1-\nu)c_n Df/\sqrt{a})}\kappa^i_{12} \\
\bar{\kappa}^i &= \sqrt{(c_n Df\sqrt{a}/2)}\kappa^i
\end{aligned} \tag{4.18}$$

then expression (4.14) is reduced to

$$\begin{aligned}
\tfrac{1}{2}c_n\{e_i\}^T[E]\{e_j\}f\sqrt{a} &= \bar{\varepsilon}^i\bar{\varepsilon}^j + \bar{\varepsilon}^i_{12}\bar{\varepsilon}^j_{12} - \bar{\varepsilon}^i_{11}\bar{\varepsilon}^j_{22} - \bar{\varepsilon}^j_{22}\bar{\varepsilon}^j_{11} \\
&\quad + \bar{\kappa}^i\bar{\kappa}^j + \bar{\kappa}^i_{12}\bar{\kappa}^j_{12} - \bar{\kappa}^i_{11}\bar{\kappa}^j_{22} - \bar{\kappa}^i_{22}\bar{\kappa}^j_{11}
\end{aligned} \tag{4.19}$$

The right-hand side of (4.19) requires only eight multiplications and is the formula actually used in the program. The multiplications involved in forming the barred quantities in (4.17) and (4.18) can be taken outside two of the do-loops and do not add significantly to the computation time.

Computing time is also saved by exploiting the fact that the bending strains do not depend on u or v in Donnell-Vlasov and shallow shell theories. Hence in these cases the bending strains can be omitted from (4.19) whenever the i-th or j-th generalized displacement relates to u or v.

5.0 Load Vector

The calculation of the load vector is quite similar to the calculation of the stiffness matrix. The formula for the virtual work per unit area of the applied loads, including thermal effects, has been given in section 2.3. The total virtual work of the loads acting on a finite element then is

$$\begin{aligned}
Ve &= \int\int(\{P\}^T\{d\} + \{Q\}^T\{e\})\sqrt{a}\,d\alpha\,d\beta \\
&= \int\int(\{P\}^T[R_d]\{d'\} + \{Q\}^T\{e\})\sqrt{a}\,d\alpha\,d\beta
\end{aligned} \tag{5.1}$$

Hence the i-th term of the load vector {L} is given by

$$\begin{aligned} \ell_i &= \partial V_e/\partial X_i \\ &= \int\int (\{P\}^T[R_d]\{d_i'\} + \{Q\}^T\{e_i\})\sqrt{a}\,d\alpha\,d\beta \end{aligned} \tag{5.2}$$

After transformation to local coordinates and evaluation by numerical integration, (5.2) becomes

$$\ell_i = \tfrac{1}{2} \sum_n c_n(\{\{P\}^T[R_d]\{d_i'\} + \{Q\}^T\{e_i\})f\sqrt{a})_n \tag{5.3}$$

To compute the above expression, values of the applied loads and temperatures must be known at each pivotal point of the numerical integration. This data is fed into the program from a user-supplied subroutine which must return the values of the three physical components of load, together with the temperature resultant and moment, at an arbitrarily given point α,β. For convenience, this subroutine and the subroutine which furnishes the values of the elastic constants are combined into one.

The technique which was used to make the calculation of the stiffness matrix more efficient is also used to simplify (5.3).

6.0 Performance of CURSHL

In this section some results which illustrate the performance and accuracy of CURSHL are presented. It goes without saying that numerous unreported tests were also run with CURSHL to check that the program functions correctly, and to discover and eliminate bugs.

6.1 Accuracy of Numerical Integration

In order to obtain some appreciation of the errors due to numerical integration the problem of a pressurized spherical cap was solved and compared with a previous solution based on the high-precision shallow shell element of Reference [7]. Both

elements use the same interpolation functions but the latter element uses exact closed-form integration, so the discrepancies between the two solutions are due entirely to errors of numerical integration in CURSHL. These discrepancies are tabulated in column B of Table VII. For comparison, the error in the finite element solution of Reference [7] is tabulated in columns A of the table. Thus columns A represent the discretization error of the high-precision elements and columns B the additional error in CURSHL due to numerical integration. In general, the latter error is small compared to the former, as expected.

The geometry of the problem is illustrated in Figure 4.

6.2 Computation Time

The time required by CURSHL to compute one stiffness matrix and load vector lies between 1.1 and 1.7 seconds depending on the nature of the shell and the choice of shell theory. More details are given in Table VIII. The times quoted were obtained on an IBM 360/67 machine under TSS (Time Sharing System). The programs had been compiled by an optimizing compiler using H level Fortran.

6.3 Rigid Body Modes

Ideally the stiffness matrix should have six zero eigenvalues, corresponding to the six rigid-body modes of the element. The smallness of the first six eigenvalues is often used as a measure of the quality of the stiffness matrix. The eigenvalues of CURSHL for a number of cases are presented in Table IX.

The first case is a flat plate, and the effect of changes in the thickness is examined. It is seen that the first six eigenvalues are satisfactorily small. Next are considered three cases where the strain-free modes can be represented by polynomial interpolation functions and hence should be exactly represented by CURSHL. The cases include a flat plate, a shallow spherical

shell, and a deep cylindrical shell using Donnell-Vlasov theory. The first six eigenvalues are again satisfactorily small in these cases. Finally cylindrical and spherical elements are considered using Koiter-Sanders deep shell theory, and the effect of changes in curvature is examined. In these cases the rigid body modes can only be approximated by polynomial interpolation functions. Here the first six eigenvalues are reasonably small if the curvature of the element is shallow but become larger as the curvature increases.

The eigenvalues quoted here differ drastically from the eigenvalues quoted in Reference [1]. The reason is that Reference [1] gives the eigenvalues of $KX = \lambda X$, K being the stiffness matrix, while Table IX gives the eigenvalues of $KX = \lambda MX$, where M is the consistent mass matrix. The computation of M follows the same general lines as the computation of K except that a 36-point numerical integration formula was used in this instance. The equation $KX = \lambda MX$ is preferred to $KX = \lambda X$ for two reasons. With the former equation the ratios of successive eigenvalues are independent of scale, and the eigenvalues have a physical interpretation in terms of natural frequencies.

For all calculations the stretching rigidity $Et/(1-\nu^2)$ and the surface mass density ρt were taken as unity, while the form of the element was a right-angled isosceles triangle with unit sides.

It may be noted from Table IX that the first eigenvalue, although always small, is sometimes negative. Therefore the stiffness matrix does not quite have the expected property of positive semi-definiteness. The negative eigenvalue is felt to be due to errors of numerical integration and possibly to round-off.

7.0 References

1. G.R. Cowper, G. M. Lindberg, M.D. Olson, "Comparison of Two High-Precision Triangular Finite Elements for Arbitrary Deep Shells", Proceedings, Third Conference on Matrix Methods in Structural Mechanics, Wright-Patterson AFB, Ohio, October 19-21, 1971.

2. A.E. Green, W. Zerna, "Theoretical Elasticity". Oxford, Clarendon Press, 1954.

3. W.T. Koiter, "A Consistent First Approximation in the General Theory of Elastic Shells." Proc. IUTAM Symposium on Theory of Thin Elastic Shells, Delft, 1959.

4. B. Budiansky, J.L. Sanders, "On the 'Best' First Order Linear Shell Theory." Progress in Applied Mechanics (The Prager Anniversary Volume), Macmillan, 1963.

5. G.R. Cowper, E. Kosko, G.M. Lindberg, M.D. Olson, "A High-Precision Triangular Plate Bending Element." National Research Council of Canada Aeronautical Report LR-514, 1968.

6. G.R. Cowper, E. Kosko, G.M. Lindberg, M.D. Olson, "Static and Dynamic Applications of a High-Precision Plate Bending Element." AIAA Journal vol. 7, pp 1957-1965, 1969.

7. G.R. Cowper, G.M. Lindberg, M.D. Olson, "A Shallow Shell Finite Element of Triangular Shape." Int'l J. Solids and Structures, vol. 6, pp 1133-1156, 1970.

8. G.M. Lindberg, M.D. Olson, "A High-Precision Triangular Cylindrical Shell Finite Element." AIAA Journal, vol.9, pp 530-532, 1971.

9. G.R. Cowper, "Gaussian Integration Formulas for Triangular Areas." In preparation.

10. G.R. Cowper, G.M. Lindberg, "A High-Precision Triangular Finite Element for Arbitrary Shells." Proceedings, Third Canadian Congress of Applied Mechanics. P.G. Glockner ed., Calgary, May 1971.

11. R.W. McLay, "Completeness and Convergence Properties of Finite Element Displacement Functions: A General Treatment," AIAA Paper No. 67-143, AIAA 5th Aerospace Sciences Meeting, New York, Jan. 1967.

12. P.G. Glockner, "Some Results on the Midsurface Deformation of Thin Shells," Proceedings, Third Canadian Congress of Applied Mechanics, Calgary, May 1971, p. 257.

Table I

Strain-Displacement Matrix [B]

$$[B] = \begin{bmatrix} B_{11} & B_{12} \\ B_{21} & B_{22} \end{bmatrix}$$

$$B_{11} = \begin{bmatrix} -\Gamma^1_{11} & 1 & 0 & -\Gamma^2_{11} & 0 & 0 \\ -\Gamma^1_{12} & 0 & \tfrac{1}{2} & -\Gamma^2_{12} & \tfrac{1}{2} & 0 \\ -\Gamma^1_{22} & 0 & 0 & -\Gamma^2_{22} & 0 & 1 \end{bmatrix} \qquad B_{12} = \begin{bmatrix} -b_{11} & 0 & 0 & 0 & 0 & 0 \\ -b_{12} & 0 & 0 & 0 & 0 & 0 \\ -b_{22} & 0 & 0 & 0 & 0 & 0 \end{bmatrix}$$

$$B_{22} = \begin{bmatrix} 0 & \Gamma^1_{11} & \Gamma^2_{11} & -1 & & 0 \\ 0 & \Gamma^1_{12} & \Gamma^2_{12} & 0 & -1 & 0 \\ 0 & \Gamma^1_{22} & \Gamma^2_{22} & 0 & 0 & -1 \end{bmatrix}$$

In Koiter-Sanders theory

$$B_{21} = \begin{bmatrix} -b^1_{1|1} + b^1_1\Gamma^1_{11} + b^2_1\Gamma^1_{12} & -b^1_1 & b_1{}^2/2 & -b^2_{1|1} + b^1_1\Gamma^2_{11} + b^2_1\Gamma^2_{12} & -3b^2_1/2 & 0 \\ (-b^1_{1|2} - b^1_{2|1} + b^1_2\Gamma^1_{11} + & -b^1_2/2 & (-3b^1_1 + b^2_2)/4 & (-b^2_{1|2} - b^2_{2|1} + b^1_2\Gamma^2_{11} + & (-3b^2_2 + b^1_1)/4 & -b^2_1/2 \\ \quad + (b^1_1 + b^2_2)\Gamma^1_{12} + b^2_1\Gamma^1_{22})/2 & & & \quad + (b^1_1 + b^2_2)\Gamma^2_{12} + b^2_1\Gamma^2_{22})/2 & & \\ -b^1_{2|2} + b^1_2\Gamma^1_{12} + b^2_2\Gamma^1_{22} & 0 & -3b^1_2/2 & -b^2_{2|2} + b^1_2\Gamma^2_{12} + b^2_2\Gamma^2_{22} & b^1_2/2 & -b^2_2 \end{bmatrix}$$

In Donnell-Vlasov and shallow shell theory, $B_{21} = 0$.

Table II

Elasticity Matrix [E]

$$[E] = \begin{bmatrix} CE_1 & 0 \\ 0 & DE_1 \end{bmatrix}$$

$$[E_1] = \begin{bmatrix} (a^{11})^2 & 2a^{11}a^{12} & (1-\nu)(a^{12})^2+\nu a^{11}a^{22} \\ 2a^{11}a^{12} & 2(1-\nu)a^{11}a^{22}+2(1+\nu)(a^{12})^2 & 2a^{22}a^{12} \\ (1-\nu)(a^{12})^2+\nu a^{11}a^{22} & 2a^{22}a^{12} & (a^{22})^2 \end{bmatrix}$$

Table III

Transformation Matrices for Tangential Displacements

$$[T_u] = \begin{bmatrix} 1 & 0 & 0 & 0 & 0 & 0 & 0 & 0 & 0 & 0 \\ 0 & 1 & 0 & 0 & 0 & 0 & 0 & 0 & 0 & 0 \\ 0 & 0 & 1 & 0 & 0 & 0 & 0 & 0 & 0 & 0 \\ -3 & -2 & 0 & 3 & -1 & 0 & 0 & 0 & 0 & 0 \\ -13 & -3 & -3 & -7 & 2 & -1 & -7 & -1 & 2 & 27 \\ -3 & 0 & -2 & 0 & 0 & 0 & 3 & 0 & -1 & 0 \\ 2 & 1 & 0 & -2 & 1 & 0 & 0 & 0 & 0 & 0 \\ 13 & 3 & 2 & 7 & -2 & 2 & 7 & 1 & -2 & -27 \\ 13 & 2 & 3 & 7 & -2 & 1 & 7 & 2 & -2 & -27 \\ 2 & 0 & 1 & 0 & 0 & 0 & 2 & 0 & 1 & 0 \end{bmatrix}$$

$$[R_u] = \begin{bmatrix} R_1 & 0 & 0 & 0 \\ 0 & R_1 & 0 & 0 \\ 0 & 0 & R_1 & 0 \\ 0 & 0 & 0 & 1 \end{bmatrix} \quad \text{where } [R_1] = \begin{bmatrix} 1 & 0 & 0 \\ 0 & f_{11} & f_{21} \\ 0 & f_{12} & f_{22} \end{bmatrix}$$

Table IV

Transformation Matrices for Normal Displacement

$$[R_W] = \begin{bmatrix} R_2 & 0 & 0 \\ 0 & R_2 & 0 \\ 0 & 0 & R_2 \end{bmatrix}$$

$$[R_2] = \begin{bmatrix} 1 & 0 & 0 & 0 & 0 & 0 \\ 0 & f_{11} & f_{21} & 0 & 0 & 0 \\ 0 & f_{12} & f_{22} & 0 & 0 & 0 \\ 0 & 0 & 0 & f_{11}^2 & 2f_{11}f_{21} & f_{21}^2 \\ 0 & 0 & 0 & f_{11}f_{12} & f_{11}f_{22}+f_{12}f_{21} & f_{21}f_{22} \\ 0 & 0 & 0 & f_{12}^2 & 2f_{12}f_{22} & f_{22}^2 \end{bmatrix}$$

Table V

Numerical Integration Formula Used in CURSHL

$$\int_{\Delta}\int f\,dxdy = A\sum_{i=1}^{13} c_i f(\xi_i,\eta_i,\zeta_i)$$

where A = area of triangle

ξ,η,ζ = area coordinates of points within triangle

i	c_i	ξ_i	η_i	ζ_i
1	-.14957 00444 67670	.33333 33333 33333	.33333 33333 33333	.33333 33333 33333
2	.17561 52574 33204	.47930 80678 41923	.26034 59660 79038	.26034 59660 79038
3	"	.26034 59660 79038	.47930 80678 41923	.26034 59660 79038
4	"	.26034 59660 79038	.26034 59660 79038	.47930 80678 41923
5	.05334 72356 08839	.86973 97941 95568	.06513 01029 02216	.06513 01029 02216
6	"	.06513 01029 02216	.86973 97941 95568	.06513 01029 02216
7	"	.06513 01029 02216	.06513 01029 02216	.86973 97941 95568
8	.07711 37608 90257	.63844 41885 69809	.31286 54960 04875	.04869 03154 25316
9	"	.63844 41885 69809	.04869 03154 25316	.31286 54960 04875
10	"	.31286 54960 04875	.63844 41885 69809	.04869 03154 25316
11	"	.04869 03154 25316	.63844 41885 69809	.31286 54960 04875
12	"	.31286 54960 04875	.04869 03154 25316	.63844 41885 69809
13	"	.04869 03154 25316	.31286 54960 04875	.63844 41885 69809

Table VI

Transformation Matrix for Generalized Displacements

$$[R_d] = \begin{pmatrix} R_3 & 0 & 0 & 0 \\ 0 & R_3 & 0 & 0 \\ 0 & 0 & R_3 & 0 \\ 0 & 0 & 0 & R_4 \end{pmatrix}$$

$$[R_3] = \begin{pmatrix} 1 & 0 & 0 \\ 0 & d_{11} & d_{21} \\ 0 & d_{12} & d_{22} \end{pmatrix} \qquad [R_4] = \begin{pmatrix} d_{11}^2 & 2d_{11}d_{21} & d_{21}^2 \\ d_{11}d_{12} & d_{11}d_{22}+d_{21}d_{12} & d_{21}d_{22} \\ d_{12}^2 & 2d_{12}d_{22} & d_{22}^2 \end{pmatrix}$$

Table VII

Comparison of Solutions for Pressurized Spherical Cap

MESH	w AT CENTRE		N_{xx} AT CENTRE		STRAIN ENERGY		M_{xx} AT CENTRE	
	A	B	A	B	A	B	A	B
1×1	2977.9	3647.2	-290.2	-33.0	-593.3	-3.3	265.7	153.4
2×2	307.8	5.9	- 19.9	- 0.18	- 63.9	-1.9	68.5	3.0
3×3	3.4	0.02	- 6.2	- 0.002	- 9.5	-0.1	6.1	0.1
MULTIPLIER	10^5 pR²/Et		10^3 pR		10^4 p²R²L²/Et		10^4 pRt	

MESH	v AT MID-EDGE		N_{xx} AT MID-EDGE		N_{yy} AT MID-EDGE		M_{xx} AT MID-EDGE	
	A	B	A	B	A	B	A	B
1×1	131.5	-14.0	28.4	1.1	94.7	3.8	88.0	-14.4
2×2	13.5	1.4	- 5.7	0.01	-18.9	0.03	16.0	0.3
3×3	1.9	0.08	- 4.3	0.001	-14.4	0.004	4.2	0.1
MULTIPLIER	10^5 pRL/Et		10^3 pR		10^3 pR		10^4 pRT	

MESH	M_{yy} AT MID-EDGE		N_{xy} AT CORNER		M_{xy} AT CORNER		
	A	B	A	B	A	B	
1×1	293.3	-48.0	-21.2	0.6	- 3.6	-3.4	
2×2	53.2	0.9	-14.1	0.03	-18.3	0.5	
3×3	13.5	0.4	- 7.0	0.001	-10.6	0.2	
MULTIPLIER	10^4 pRt		10^2 pR		10^3 pRT		

Columns A are errors of finite element solution of Reference [7].

Columns B are differences between solution of Reference [7] and CURSHL solution.

Table VIII

Computing Times for CURSHL

Shape	Theory	VMR time, sec.
flat plate	shallow	1.1
flat plate	K-S	1.2
circular cylinder	D-V	1.1
circular cylinder	K-S	1.4
sphere	D-V	1.3
sphere	K-S	1.6
elliptic cylinder	K-S	1.4
cone	K-S	1.5

Table IX

Eigenvalues of KX = λMX, where K is the CURSHL stiffness matrix

(a) Flat plate element; effect of thickness

EIGENVALUE	t = 0.2	t = 0.02	t = 0.002
λ_1	-0.71×10^{-14}	-0.70×10^{-14}	-0.70×10^{-14}
λ_6	0.70×10^{-14}	0.71×10^{-14}	0.71×10^{-14}
λ_7	0.13×10^{1}	0.13×10^{-1}	0.13×10^{-3}
λ_{36}	0.15×10^{4}	0.32×10^{3}	0.32×10^{3}
λ_6/λ_7	0.56×10^{-14}	0.56×10^{-12}	0.56×10^{-10}

(b) Cases where exact zero eigenvalues are expected, t=0.02; R=1

EIGENVALUE	FLAT PLATE	SHALLOW SPHERE	CYLINDER, D-V THEORY
λ_1	-0.70×10^{-14}	-0.11×10^{-13}	-0.76×10^{-14}
λ_6	0.71×10^{-14}	0.80×10^{-14}	0.77×10^{-14}
λ_7	0.13×10^{-1}	0.14×10^{-1}	0.14×10^{-1}
λ_{36}	0.32×10^{3}	0.41×10^{3}	0.32×10^{3}
λ_6/λ_7	0.56×10^{-12}	0.59×10^{-12}	0.55×10^{-12}

...(cont'd)

(c) Circular cylinder, Koiter-Sanders Theory; t = 0.02

EIGENVALUE	R = 10	R = 3	R = 1
λ_1	-0.98×10^{-14}	0.22×10^{-15}	-0.60×10^{-15}
λ_6	0.42×10^{-9}	0.31×10^{-6}	0.42×10^{-4}
λ_7	0.13×10^{-1}	0.13×10^{-1}	0.14×10^{-1}
λ_{36}	0.32×10^{3}	0.32×10^{3}	0.32×10^{3}
λ_6/λ_7	0.33×10^{-7}	0.24×10^{-4}	0.30×10^{-2}

(d) Spherical shell, Koiter-Sanders theory; t = 0.02

EIGENVALUE	R = 10	R = 5	R = 2
λ_1	0.25×10^{-16}	0.60×10^{-13}	0.28×10^{-9}
λ_6	0.71×10^{-8}	0.42×10^{-6}	0.84×10^{-4}
λ_7	0.13×10^{-1}	0.14×10^{-1}	0.18×10^{-1}
λ_{36}	0.32×10^{3}	0.32×10^{3}	0.34×10^{3}
λ_6/λ_7	0.54×10^{-6}	0.29×10^{-4}	0.46×10^{-2}

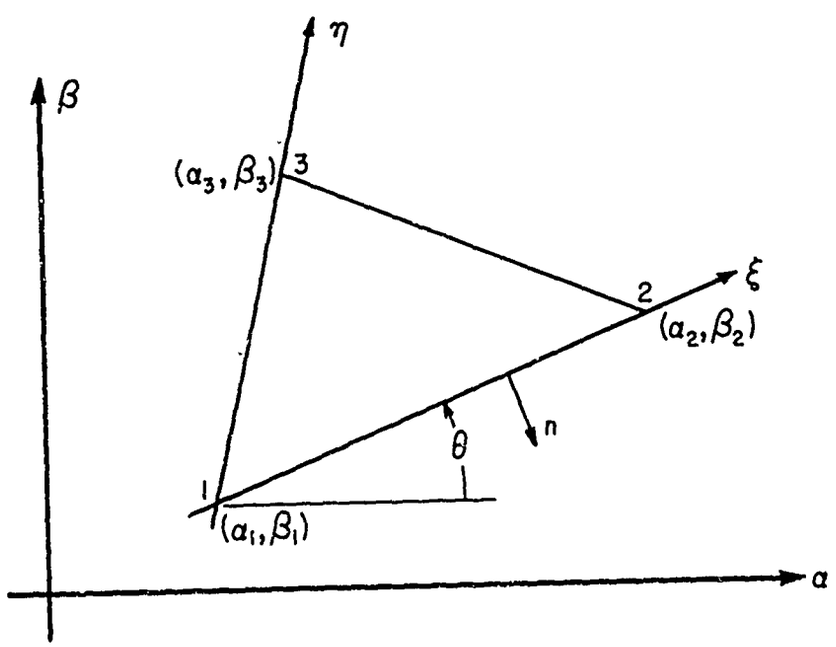

FIG. 1 LOCAL COORDINATES

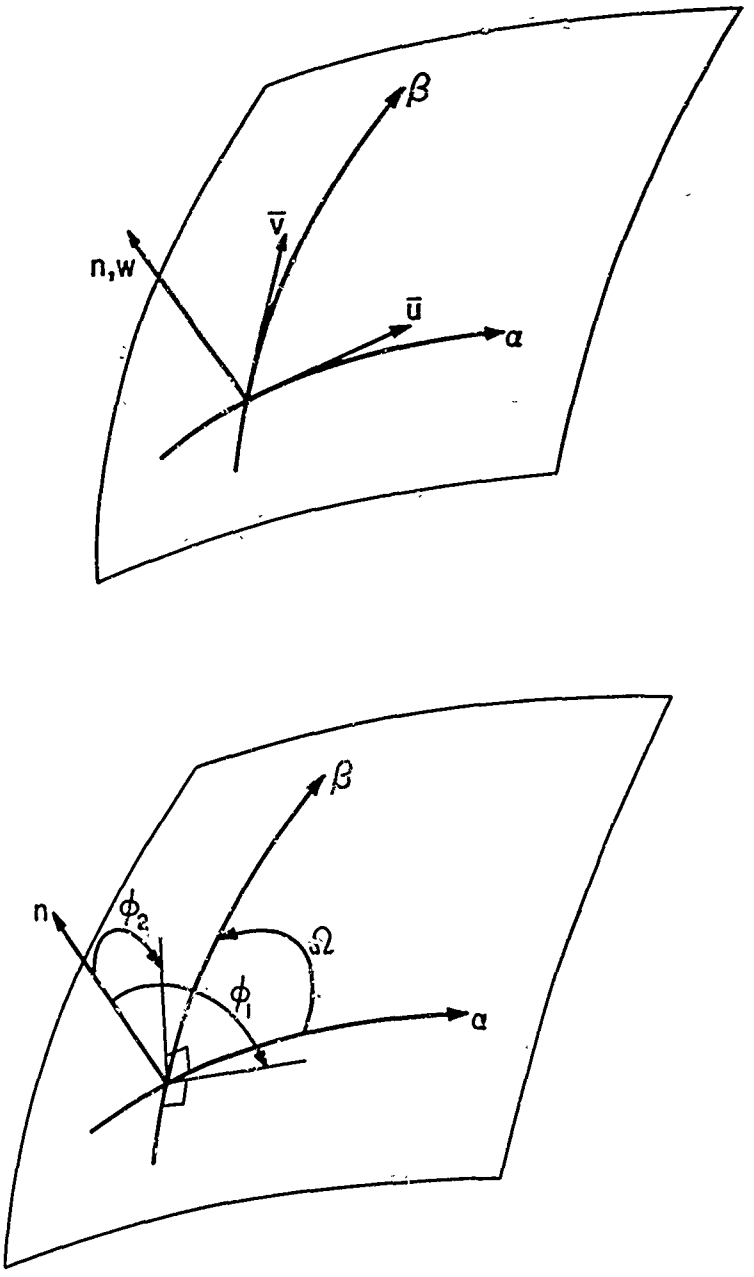

FIG. 2 POSITIVE DIRECTION OF PHYSICAL COMPONENTS OF DISPLACEMENT AND ROTATION

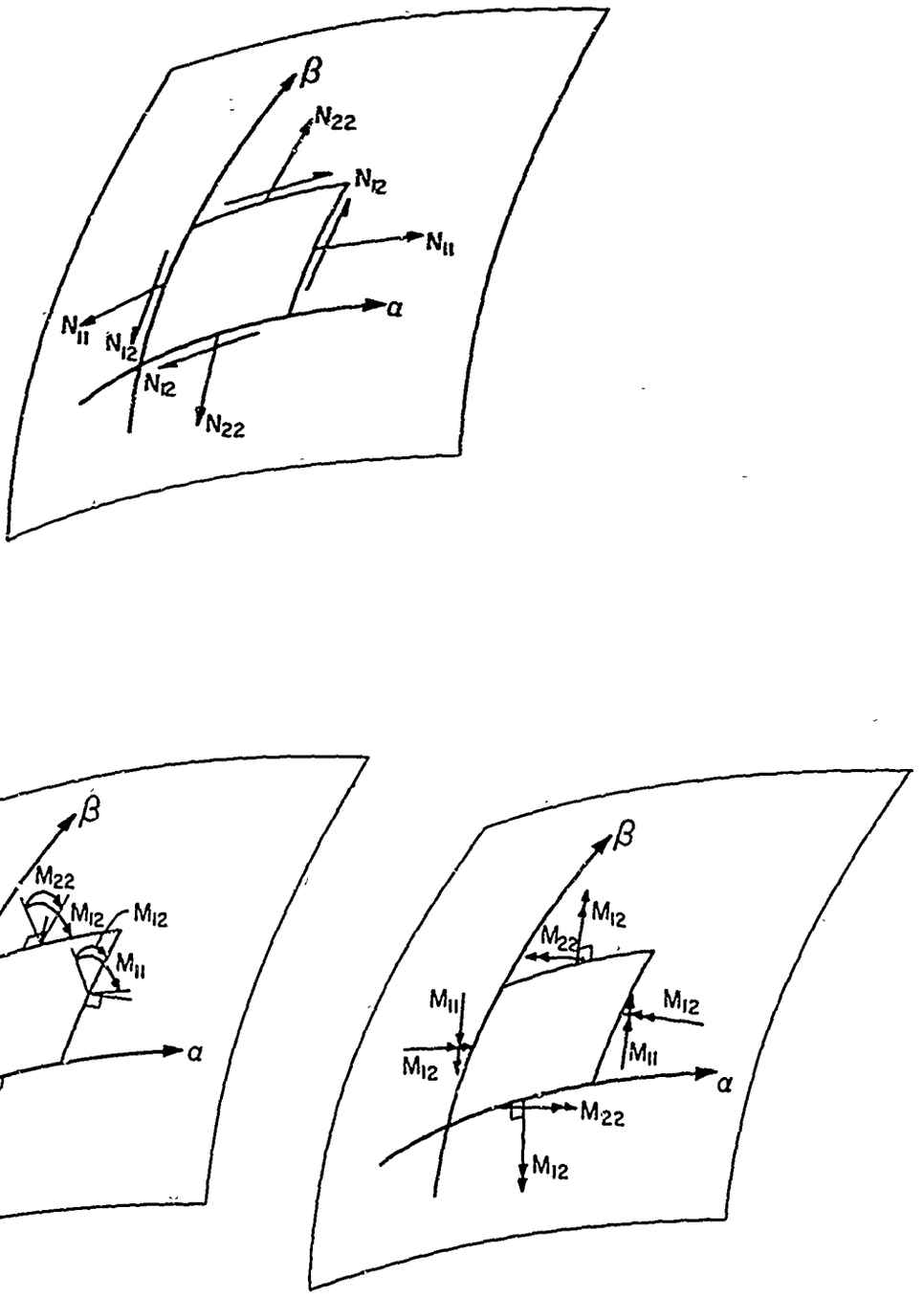

FIG. 3 POSITIVE DIRECTIONS OF PHYSICAL COMPONENTS OF STRESS RESULTANTS AND BENDING MOMENTS

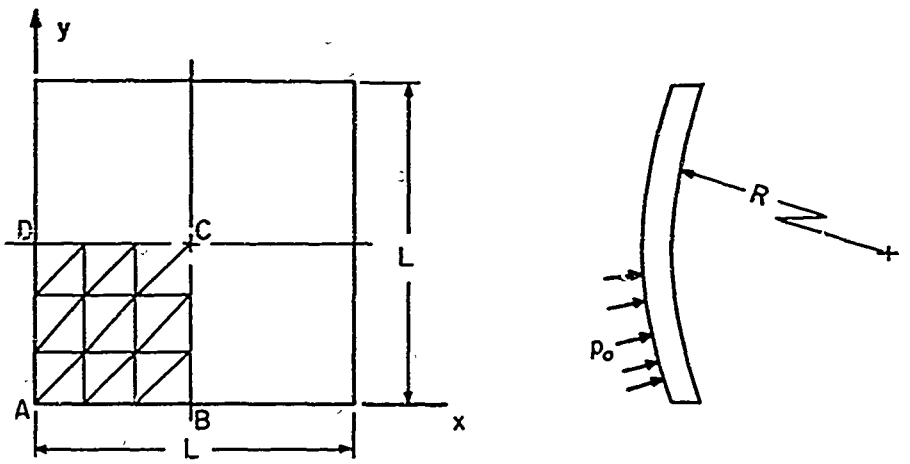

FIG. 4 DIAGRAM OF SPHERICAL CAP. UNIFORM APPLIED PRESSURE. ALL EDGES SIMPLY SUPPORTED
$Rt/L^2 = 0.02$